Room temperature multiferroic properties of single-phase $(Bi_{0.9}La_{0.1})FeO_3-Ba(Fe_{0.5}Nb_{0.5})O_3$ solid solution ceramics

Hanjong Paik,[a] Hosung Hwang, and Kwangsoo No
Department of Material Science & Engineering, Korea Advanced Institute of Science and Technology, Daejeon 305-701, Republic of Korea

Seunghwa Kwon and David P. Cann
Faculty of Materials Science, Department of Mechanical Engineering, Oregon State University, Corvallis, Oregon 97331

(Received 6 September 2006; accepted 21 December 2006; published online 24 January 2007)

The crystal structure and multiferroic properties of single-phase $(Bi_{0.9}La_{0.1})FeO_3-Ba(Fe_{0.5}Nb_{0.5})O_3$ ceramics were investigated. The rhombohedral-type structure of $1.0(Bi_{0.9}La_{0.1})FeO_3)$ was transformed to a monoclinic-type structure for the $0.5(Bi_{0.9}La_{0.1})FeO_3-0.5Ba(Fe_{0.5}Nb_{0.5})O_3)$ composition. It shows the coexistence of ferroelectricity and magnetism at room temperature, represented by a high dielectric constant with ferroelectric hysteresis and clear magnetic hysteresis behavior. The authors propose that the solid solution of A and B site cations according to their ionic radii and valence state stabilized the spontaneous polarization and magnetization at room temperature. © *2007 American Institute of Physics*. [DOI: 10.1063/1.2434182]

A significant amount interest has been noted in multiferroic materials because of the coexistence of ferroelectric and ferromagnetic ordering at room temperature.[1] The coupling effect between the magnetic domains and ferroelectric domains can be utilized via the magnetoelectric (ME) effect.[2,3] This ME effect provides an additional degree of freedom in the design of actuators, transducers, and next generation memory devices. However, the existence of ferroelectricity and ferromagnetism is usually mutually exclusive because they require empty and partially filled transition metal orbital, respectively.[4]

$BiFeO_3$ (BFO) is well known perovskite compound possessing displacement-type ferroelectric ordering ($T_C \sim 840\ ^\circ C$) and canted spin aligned antiferromagnetic ordering ($T_N \sim 340\ ^\circ C$) simultaneously.[5] Unfortunately, the relatively high leakage current, unwanted secondary phases, and other defects in BFO ceramics make it difficult to obtain a well saturated polarization and magnetization at room temperature.[6] In order to overcome the deficiencies of BFO, we have focused on the solid solution system of La-doped BFO (BLFO) with a partially *B*-site ordered $A(B_IB_{II})O_3$ double perovskite, specifically $Ba(Fe_{0.5}Nb_{0.5})O_3$ (BFNO). BFNO was chosen because it exhibits magnetic ordering through indirect exchange through ions such as Fe^{3+} on the octahedral B_I site and high dielectric constant of $\varepsilon_r \approx 10^4-10^5$ at a low frequency region.[7] Also, BFNO is well matched with BLFO due to its partially disordered *B*-site structure and manifold magnetism according to their *B*-site valence state and ionic radii.[8,9] In this letter, we report the synthesis, structural variation according to the composition, and ferroelectric/ferromagnetic properties of BLFO-BFNO ceramic solid solutions at room temperature.

The $x\ (Bi_{0.9}La_{0.1})FeO_3-(1-x)\ Ba(Fe_{0.5}Nb_{0.5})O_3$ ($x=1.0$, 0.8, and 0.5) solid solutions were prepared via solid state reaction using a temperature programmable box furnace (Fisher Scientific). High purity oxide and carbonate (above 99.9% purity of Bi_2O_3, La_2O_3, Fe_2O_3, $BaCO_3$, and Nb_2O_5) powders were weighed in stoichiometric proportions and thoroughly ball milled for 24 h using zirconium media with ethanol in a plastic jar and dried. All powders were calcined at 830–1000 °C for 3 h in an alumina crucible and milled again. Sintering was performed at 860–1050 °C for 5 h using a double crucible configuration after pelletization followed by cold pressing and cold isostatic pressing. The sample diameter was 9 ± 0.2 mm and the thickness was mechanically reduced to 0.6 ± 0.03 mm to facilitate electrical measurements.

X-ray diffraction (XRD) was used to verify the crystal structure and phase purity by step scan mode (0.05 step per 5 s from 10° to 119.95°). There were no secondary phases such as $Bi_{36}Fe_2O_{57}$, $Bi_{12}(Bi_{0.5}Fe_{0.5})O_{19.5}$, $Bi_2Fe_4O_9$, or $Bi_{46}Fe_2O_{72}$ after sintering.[10] XRD patterns were indexed by the standard computer program JADE using the appropriate PDF cards, and the nonlinear least squares method was utilized with the UNITCELL program to verify the structural variations at high BFNO compositions.[11] The grain size and surface uniformity of fresh fracture surfaces were examined by scanning electron microscopy (SEM). Energy dispersive x-ray spectroscopy (EDXS) analysis was used to verify the overall chemical homogeneity and composition. Dielectric characterization was performed at room temperature using an impedance analyzer over the frequency range from 10^2 to 10^7 Hz (HP-4192A, Hewlett-Packard). Ferroelectric hysteresis measurements were carried out at room temperature with a standardized ferroelectric system (RT66A, Radiant technologies). Magnetic hysteresis measurements were performed on a vibrating sample magnetometer (VSM) at room temperature.

Figure 1 shows the step scanned XRD patterns 1-(1) and detailed scans 1-(2) and 1-(3) for (a) 1.0BLFO, (b) 0.8BLFO-0.2BFNO, and (c) 0.5BLFO-0.5BFNO. The crystal structure of 1.0BLFO was well matched and indexed with a Powder Diffraction File (Ref. 12) for $BiFeO_3$. The calculated lattice parameters closely matched the published values for 1.0BLFO with *a* and *c* measured at 5.578 and 6.931 Å, respectively.[13,14] However, as the mole fraction of BFNO content increased, the crystal structure of the 0.5BLFO-

[a]Author to whom correspondence should be addressed; electronic mail: interkru2003@kaist.ac.kr

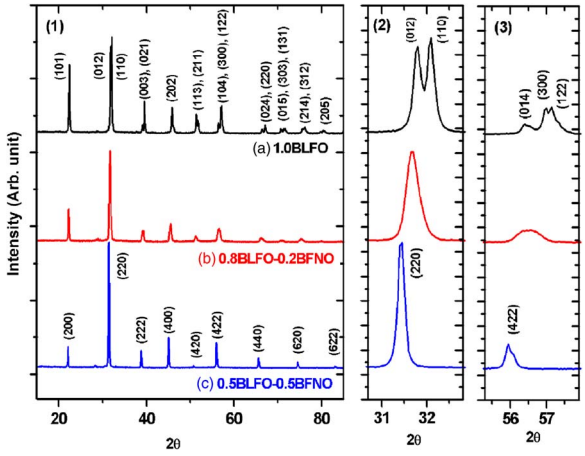

FIG. 1. (Color online) X-ray diffraction pattern 1-(1) of sintered ceramics (a) $1.0(Bi_{0.9}La_{0.1})FeO_3$, (b) $0.8(Bi_{0.9}La_{0.1})FeO_3-0.2Ba(Fe_{0.5},Nb_{0.5})O_3$, and (c) $0.5(Bi_{0.9}La_{0.1})FeO_3-0.5\ Ba(Fe_{0.5},Nb_{0.5})O_3$, and their detailed scans 1-(2) and 1-(3).

0.5BFNO solid solution showed a close match to a monoclinic-type structure. The unit cell parameters of 0.5BLFO-0.5BFNO were calculated as $a=8.052$, $b=8.046$, $c=8.069$ Å, and $\beta=90.023$ ° based on a Powder Diffraction File (Ref. 15) for $Ba(Fe_{0.33}Nb_{0.67})O_3$ as similar to the 1.0BFNO structure.[7] Moreover, the detailed diffraction patterns of Figs. 1(b) and 1(c) clearly confirm the structural variations as a function of BFNO content. The calculated cell parameters are summarized in Table I.

SEM images of fresh fracture surfaces in Figs. 2(a) 1.0BLFO, 2(b) 0.8BLFO-0.2BFNO, and 2(c) 0.5BLFO-0.5BFNO show a dense microstructure with well defined grains with no segregation of impurities. The EDXS analysis verified the chemical homogeneity of each sample. While the (a) 1.0BLFO and (b) 0.8BLFO-0.2BFNO samples had a grain size of about 1–2 μm, that of (c) 0.5BLFO-0.5BFNO was enlarged to around 5–8 μm. This grain enlargement could be responsible for the higher dielectric constant at the composition (c) 0.5BLFO-0.5BFNO.

The frequency dependence of the relative permittivity and loss tangent is represented in Fig. 3(a) 1.0BLFO, 3(b) 0.8BLFO-0.2BFNO, and 3(c) 0.5BLFO-0.5BFNO over the frequency range from 10^2-10^7 Hz at room temperature. The relative permittivity of (a) 1.0BLFO displayed a weak frequency dependence; however, the compositions (b)

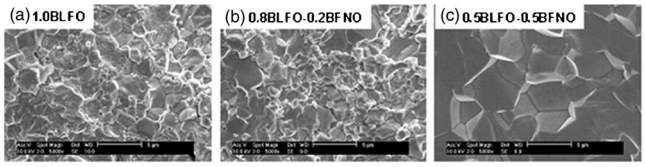

FIG. 2. Scanning electron microscope of fracture surface (a) $1.0(Bi_{0.9},La_{0.1})FeO_3$, (b) $0.8(Bi_{0.9},La_{0.1})FeO_3-0.2Ba(Fe_{0.5},Nb_{0.5})O_3$, and (c) $0.5(Bi_{0.9},La_{0.1})FeO_3-0.5\ Ba(Fe_{0.5},Nb_{0.5})O_3$.

0.8BLFO-0.2BFNO and (c) 0.5BLFO-0.5BFNO display significant frequency dispersion behavior which is likely due to nonstoichiometric effects.[10] There is also large fluctuation in dielectric permittivity of (c) 0.5BLFO-0.5BFNO compared to the other samples, which may be attributed to space charge effects.[16]

We have also attempted to measure ferroelectric hysteresis at room temperature, as shown in Fig. 4. There is a formation of a well-defined nonlinearity in the hysteresis loop and a clear modification in the ferroelectric behavior with BFNO additions. The loops are not fully saturated due to the limitation of our measurement system. Also, ferroelectric hysteresis loops observed by Holland and Redfern[11] did not show any saturation even at a temperature of 80 K.[11]

The as-prepared ceramic clearly demonstrated a spontaneous magnetization at room temperature, as shown in Fig. 5. Especially, the (c) 0.5BLFO-0.5BFNO composition represented a large enhancement in the magnetization. The coercive field (H_c) and remanent magnetization (M_r) of each sample were (a) 10.737 kOe, 2.046 memu/g, (b) 2.911 kOe, 64.813 memu/g, and (c) 3.125 kOe, 539.090 memu/g, respectively. Structural modifications with increased BFNO contents would likely be responsible for the observed enhanced magnetization at room temperature. Specially, the diminished magnetic properties of both H_c and M_r in 1.0BLFO is due to the space-modulated spin structure, which is transformed to an arranged spin moment according to the monoclinic-type structure in the BFNO rich sample. A more detailed analysis of the magnetic properties as a function of temperature is in progress.

In summary, the perovskite solid solution of BFNO with BLFO was demonstrated to exhibit room temperature multiferroism. By manipulating the *A*-site and *B*-site cation ordering in this complex perovskite, a spontaneous polarization and large magnetic moment could be achieved at room tem-

TABLE I. Unitcell information calculated by least square method for $1.0(Bi_{0.9},La_{0.1})FeO_3$ and $0.5(Bi_{0.9},La_{0.1})FeO_3$-0.5 $Ba(Fe_{0.5},Nb_{0.5})O_3$.

Materials	Parameters	Value	Structure	95% confidence	Residuals (sigmafit)	Remarks
1.0BLFO	a (Å)	5.579 16	Rhombohedral	0.000 27	5.4989	Ref. 13 Ref. 14
	(Å)	6.930		0.001 01		
	Cell vol. (Å^3)	186.8170		0.025 9		
0.5BLFO-0.5BFNO	a (Å)	8.052	Monoclinic	0.000 56	2.2476	Ref. 7 Ref. 8 Ref. 9
	b (Å)	8.046		0.002 11		
	c (Å)	8.059		0.005 72		
	β (deg)	90.023		0.031 39		
	Cell vol. (Å^3)	522.115		0.374 4		

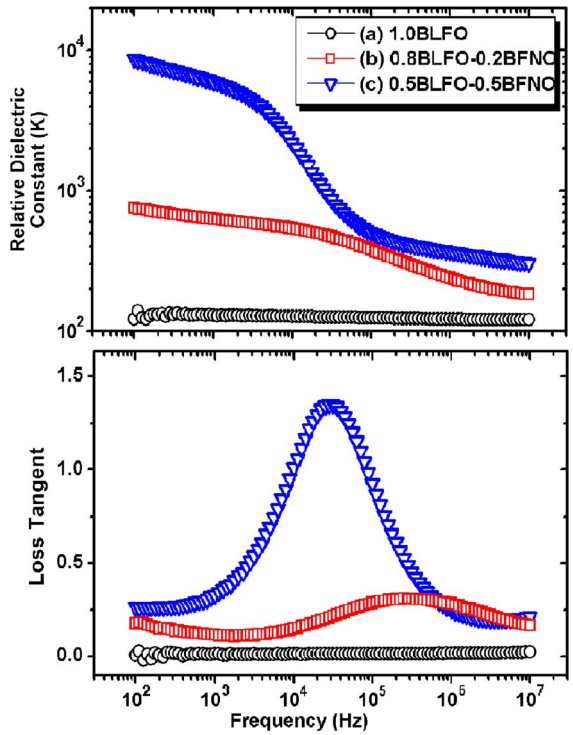

FIG. 3. (Color online) Relative permittivity and loss tangent of the sintered ceramics (a) $1.0(Bi_{0.9},La_{0.1})FeO_3$, (b) $0.8(Bi_{0.9},La_{0.1})FeO_3-0.2Ba(Fe_{0.5},Nb_{0.5})O_3$, and (c) $0.5(Bi_{0.9},La_{0.1})FeO_3-0.5\ Ba(Fe_{0.5},Nb_{0.5})O_3$ at a frequency range from 10^2 to 10^7 Hz.

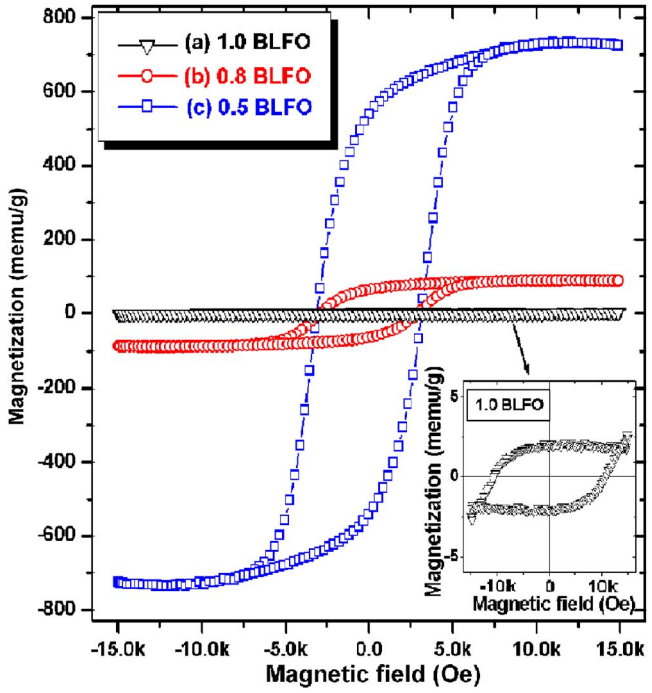

FIG. 5. (Color online) Magnetization vs magnetic field hysteresis loop of the sintered ceramics (a) $1.0(Bi_{0.9},La_{0.1})FeO_3$, (b) $0.8(Bi_{0.9},La_{0.1})FeO_3-0.2Ba(Fe_{0.5},Nb_{0.5})O_3$, and (c) $0.5(Bi_{0.9},La_{0.1})FeO_3-0.5\ Ba(Fe_{0.5},Nb_{0.5})O_3$ measured at room temperature. Inset figure shows magnified *M-H* hysteresis for (a) $1.0(Bi_{0.9},La_{0.1})FeO_3$.

perature. An enhanced net magnetization was realized through an uncompensated antiferromagnetic moment owing to structural distortion and cation ordering. The ceramic undergoes a frequency dispersed dielectric property with a spontaneous polarization of 0.3 $\mu C/cm^2$ and magnetization of 539 memu/g at room temperature.

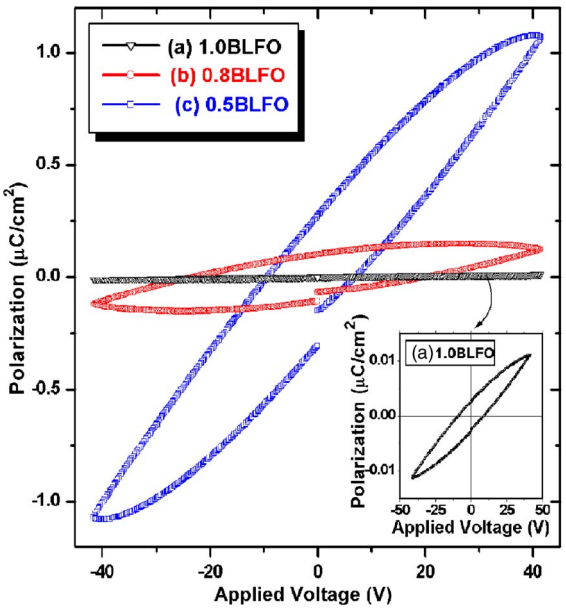

FIG. 4. (Color online) Polarization vs applied voltage hysteresis of the sintered ceramics (a) $1.0(Bi_{0.9},La_{0.1})FeO_3$, (b) $0.8(Bi_{0.9},La_{0.1})FeO_3-0.2Ba(Fe_{0.5},Nb_{0.5})O_3$, and (c) $0.5(Bi_{0.9},La_{0.1})FeO_3-0.5\ Ba(Fe_{0.5},Nb_{0.5})O_3$ measured at room temperature. Inset figure shows magnified *P-V* hysteresis for (a) $1.0(Bi_{0.9},La_{0.1})FeO_3$.

This work was supported by the Korea Research Foundation Grant funded by the Korean Government (MOEHRD, KRF-2006-C00135-I00713), and partially supported by the Ministry of Education in Korea (project named "Brain Korea 21"). The authors also appreciated the VSM measurement to Sang-Hwan Park in Magnetic Thin Films Laboratory, KAIST, Korea.

[1]N. A. Spaldin and M. Fiebig, Science **309**, 391 (2005).
[2]M. Fiebig, J. Phys. D **38**, R123 (2005).
[3]W. Prellier, M. P. Singh, and P. Murugavel, J. Phys.: Condens. Matter **17**, R803 (2005).
[4]M. M. Kumar, V. R. Palkar, K. Srinivas, and S. V. Suryanarayana, Appl. Phys. Lett. **76**, 2764 (2000).
[5]J. Wang, J. B. Neaton, H. Zheng, V. Nagarajan, S. B. Ogale, B. Liu, D. Viehland, V. Vaithyanathan, D. G. Schlom, U. V. Waghmare, N. A. Spaldin, K. M. Rabe, M. Wuttig, and R. Ramesh, Science **299**, 1719 (2003).
[6]Y. K. Jun, W. T. Moon, C. M. Chang, H. S. Kim, H. S. Ryu, J. W. Kim, K. H. Kim, and S. H. Hong, Solid State Commun. **135**, 133 (2005).
[7]N. Rama, J. B. Philipp, M. Opel, K. Chandrasekaran, V. Sankaranarayaran, R. Gross, and M. S. Ramachandra Rao, J. Appl. Phys. **95**, 7528 (2004).
[8]Sonali Saha and T. P. Shina, J. Phys.: Condens. Matter **14**, 249 (2002).
[9]Keitaro Tezuka, Kou Henmi, Yukio Hinatsu, and Nobuyuki M. Masaki, J. Solid State Chem. **154**, 591 (2000).
[10]X. Qi, J. Dho, R. Tomov, M. G. Blamire, and J. L. MacManus-Driscoll, Appl. Phys. Lett. **86**, 062903 (2005).
[11]T. J. B. Holland and S. A. T. Redfern, Miner. Mag. **61**, 65 (1997).
[12]PDF No. 20-0169 (unpublished).
[13]V. R. Palkar, D. C. Kundaliya, S. K. Malik, and S. Bhattacharya, Phys. Rev. B **69**, 212102 (2004).
[14]I. Sosnowska, R. Przenioslo, P. Fischer, and V. A. Murashov, J. Magn. Magn. Mater. **160**, 384 (1996).
[15]PDF No. 17-0187 (unpublished).
[16]M. Mahesh Kumar, V. R. Palker, K. Srinivas, and S. V. Suryanarayana, Appl. Phys. Lett. **76**, 2764 (2000).